

Target Recognition Based on Mathematical Morphology

Zuoping Chen
School of Science
Northwestern Polytechnical University
Xi'An, China 710072
Email: chanzuoping@hotmail.com

David T. W. Chan
Industrial Centre
The Hong Kong Polytechnic University
Hung Hom Kowloon, Hong Kong
ictwchan@inet.polyu.edu.hk

Zhenglin Ye
School of Science
Northwestern Polytechnical University
Xi'An, China 710072
Email: yezhenln@nwpu.edu.cn

Guohua Peng
School of Science
Northwestern Polytechnical University
Xi'An, China 710072
Email: penggh@nwpu.edu.cn

Abstract

A recognition algorithm for a type of coded target widely used in photogrammetry is presented in this paper. An efficient feature vector is first proposed to describe the targets, then mathematical morphological operations are used for clustering to location the targets in the image. Finally, by ellipse fitting, each coded target in the image is recognized. Experimental results in both the better and worse case demonstrate the effectiveness of our approach.

1. Introduction

3D Object modeling has become a hot issue in many fields such as computer graphics, computer vision and reverse engineering in recent years. For acquisition of the 3D data of the object surface, noncontact survey based on digital cameras is showing its advantages over the traditional contact methods such as the Coordinate Measuring Machine (CMM) with lower cost, higher speed and bigger range [5]. In this method, to obtain the point cloud data of the object surface, some special landmarks as reference points are often attached to a frame associated with the object or directly to smooth regions of the object, then several photos are taken from different viewpoints. By photogrammetry theory, the 3D coordinates of the points on the object surface can be recovered if there exist at least three common landmarks in two photos. Furthermore, these common landmarks will greatly facilitate registration of the two multiview point clouds into a single representation, since they provide a good correspondence between the two point

clouds [1].

Apparently, the operations above all depend on the recognition of the landmarks. Although great efforts have been made on the registration of multiview point clouds, landmark recognition receives few attention. As to our knowledge, the only publication was proposed by Ma and Xing in [4], where another type of landmark is recognized using some invariant moments, with no results about the running time or the recognition rate provided, however.

Mathematical Morphology is a set-theoretic method of image analysis providing a quantitative description of geometrical structures with some morphological set transformations such as *dilation*, *erosion*, *opening* and *closing*. Details are referred to [7]. This paper presents an algorithm for recognition of a type of widely used landmark designed by AICON Co., based on the mathematical morphology.

2 Proposed algorithm for code targets

2.1 Representation and classification of the coded targets

Various landmarks have been used for 3D measurement at present. In this paper, we focus on the one designed by AICON Co. (called *coded target*), which has been widely used in photogrammetry. An illustration is shown in Fig.1. A *target* consists of a central circle and an outer cirque, with the circle's radius and the cirque's width being 4.5mm and 4mm respectively, and the distance between them being 6mm. The cirque is evenly partitioned into 14 parts, each of which is called a *unit*. We might as well call the target with 14 units the *full target* (Fig.1(a)). A *coded target* in use is a

target with some units removed from the outer cirque with a assigned natural number, called its *code*. For example, the coded target shown as Fig.1(b) is coded by 105.

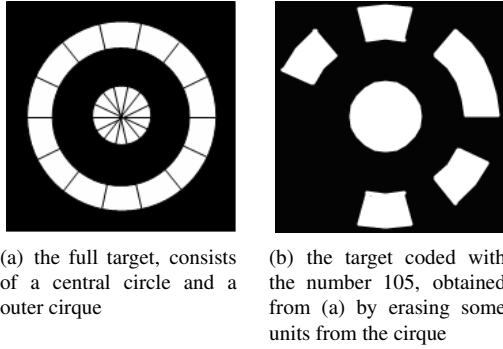


Figure 1. Illustration of the coded targets designed by AICON Co.

Given a clock direction, each coded target can be represented by an interlacing sequence

$$W_1 B_1 W_2 B_2 \cdots W_m B_m \quad (1)$$

where $1 \leq W_i, B_i \leq 14$ are the numbers of units in i th separate white and black parts in the cirque respectively, and m the number of white or black parts. An Efficient expression is to use a lowercase among 'a' to 'n' to denote the number of units occupied by a white part, and an uppercase among 'A' to 'N' by a black part. Thus the target in Fig.1(b) can be represented by the sequence "DaAaAbAaAa".

It's should be mentioned that when we truncate the sequence above at any possible position (this corresponds to different start-point when counting the parts) into two subsequences and exchange them, we obtain a new sequence which also represent the same coded target. Therefore, before the recognition, we need to store for each coded target the pair

$$(code, sequence) \quad (2)$$

where *sequence* is the so-called *standard* sequence of the target. Any other sequence representing the same target can be considered as *homeomorphous* sequences since they can be recovered by the standard one with truncation and exchanging. Furthermore, to speed up the recognition, we classify all the targets into at most 14 categories, based on the number of separate white or black parts in the outer cirque. For example, the target shown in Fig.1(b) is put into the fifth category.

For a coded target in recognition, once one of its homeomorphous sequence is figured out, the comparisons are then executed under the truncation and exchanging operation between this sequence and the standard sequences of all targets from the corresponding class, until it matches someone,

when the corresponding code number is extracted from the stored pair (*code*, *sequence*).

2.2 Clustering by morphology

For an image containing targets, the first thing is to position the targets in the image. Although the targets in the image often dominate the other contents in the sense of intensity, there are still many noises due to the imaging environment or some components of the object with similar intensities to that of the targets nearby. An example is shown in Fig.2(a), which is a portion of the image of the vacuum flask. Thus methods are required to eliminate the noise and separate the targets from each other, i. e., a "clustering" with each target as a cluster is needed. There have been many clustering algorithms at present, most of which based on density [3] [6] or distance [2]. However, the selection of the density or distance threshold is often a disturbing problem. Furthermore, these methods may lead to wrong classification when the noise is adjacent to a target since they may take the noise as a part of the target. Hence, we propose the following algorithm for clustering based on mathematical morphology:

step1 Binarization of the original image, shown in Fig.2(b). Attention should be paid since too big intensity thresholds may lead to the lose of targets and too small ones lead to big noises.

step2 Denoising with the opening operation. From Fig.2(c) we can see the elimination of noises.

step3 Performing the dilation repeatedly until all separated white parts (including the central circle) of the targets are merged as a whole, see Fig.2(d). We might as well call the number of dilations the "dilation parameter" of the algorithm. Apparently, it is much easier to determine than the threshold used in the density or distance-based methods since the latter is a real number.

step4 Filling small gaps in the image resulted from last step using the closing operation, shown in Fig.2(e).

step5 Extracting the edge of each subregion containing a target using some region-tracing algorithm, shown in Fig.2(f), which is then used for further recognition in the next section.

2.3 Target recognition by ellipse fitting

Having obtained the edge of the subregion each target belongs to, the following loop for each edge is conducted. An ellipse fitting is necessary since some targets may be distorted due to the viewpoints in imaging.

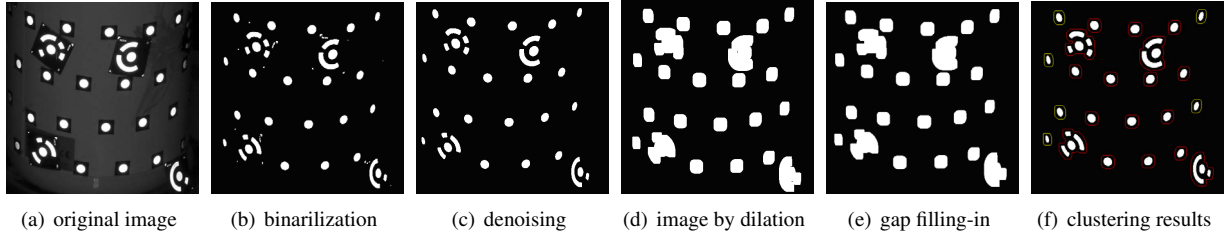


Figure 2. Clustering of the targets by thresholding and mathematical morphology

step1 Scan the corresponding subregion the edge envelopes and obtain all the subedges of the white parts in the subregion, denoted by e_1, e_2, \dots, e_m , where m is the number of subedges. If $m = 1$, break the loop.

step2 Each subedge is used for least square fitting to an ellipse with the parameters (x_c, y_c, a, b, θ) , where (x_c, y_c) denotes the center coordinates of the ellipse, a and b the half length of the long axis and short axis respectively, θ the angle between the long axis and x axis. The one with minimum fitting error is then considered as the central circle of the target.

step3 Determine the number sequence of units each part in the cirque possesses by the following procedure.

Firstly, find out two intersection points between each part and a homocentric “test” ellipse with the half length of long and short axis being $2.78a$ and $2.78b$ respectively. These two points lie at different sides of the line from center of the circle to the center of the part and are the nearest points to the test ellipse. It is also demonstrated in Fig.3. We denote the sequence of intersection points as $\mathbf{p}_1, \mathbf{p}_2, \dots, \mathbf{p}_{2m-1}, \mathbf{p}_{2m}$.

Secondly, perform the rotation on the point sequence above with a degree of θ , followed by a scaling along y axis with the factor of a/b . The transformed sequence is then denoted by $\tilde{\mathbf{p}}_1, \tilde{\mathbf{p}}_2, \dots, \tilde{\mathbf{p}}_{2m-1}, \tilde{\mathbf{p}}_{2m}$.

Thirdly, calculate the angle sequence

$$\phi_i = \angle(\mathbf{c}\tilde{\mathbf{p}}_i, \mathbf{c}\tilde{\mathbf{p}}_{i+1}), i = 1, 2, \dots, 2m, \quad (3)$$

$$\tilde{\mathbf{p}}_{2m+1} := \tilde{\mathbf{p}}_1 \quad (4)$$

where $\mathbf{c}\tilde{\mathbf{p}}_i$ is the vector from \mathbf{c} to $\tilde{\mathbf{p}}_i$.

Finally, compute the number of units each part in the cirque possess using the formula below

$$n_i = \lfloor \frac{14 \times \phi_i}{2\pi} + 0.5 \rfloor, i = 1, 2, \dots, 2m. \quad (5)$$

It is easily to know that $n_{2j}, j = 1, 2, \dots, m$ denotes the number of units belong to the parts removed from the full target, i. e., the black parts in the cirque.

step4 Constructing the homeomorphous sequence according to the unit number sequence above, which is then used for comparison with the standard sequences under the truncation and exchanging operations, hence obtaining the code of the target.

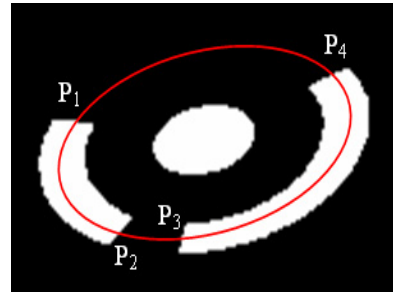


Figure 3. Intersection between each outer parts and the test ellipse

3 Experimental results

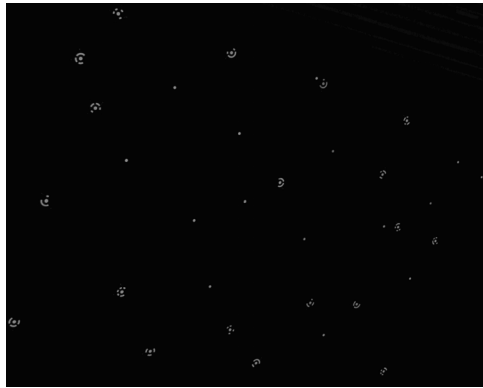
35 greyscale images of size $3024 \times 2016 \times 8$ have been tested, two of which are shown in Fig.4 and Fig.5. (for display purpose, the original images have been trimmed and scaled, but all the targets in original images are preserved.) The first one represents the better-case, i.e., with little noise and sparse distribution of the targets, which is easier to deal with. While the second one (stands for the worse case) is much more difficult to process, with a complicated background and a dense distribution of the targets.

All reported running times are for a C++ implementation running on a 1.86 GHz Pentium IV Intel processor. The results are shown in Table1. One can see that the targets in the worse-case are bigger than those in the better-case, which means more dilations are needed in step3 in section 3.2, hence more time is needed.

Table 1. Recognition results

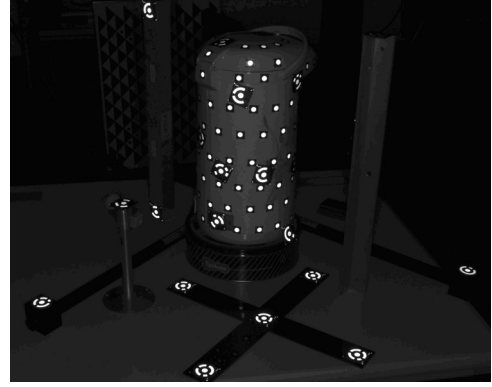
	N_D	N_{total}	$N_{detected}$	$Time(s)$
better-case	4	19	19	3.7
worse-case	6	17	16	7.2

where N_D denotes the number of dilations used in algorithm, N_{total} the number of targets in total in the image, and $N_{detected}$ the number of targets recognized by the proposed algorithm. From the table, we see that in the better case all the targets are identified correctly. As to the worse case, there is only one target in the top of the vacuum flask not recognized, since it has been too seriously distorted in shape and color. For comparison, we also used two commercial software: AICON and PhotoModeler for the recognition of the same test images. The same recognition rates are obtained, while as to the running time, the proposed algorithm is inferior to AICON with 1.5s on average and very similar to PhotoModeler. However, in PhotoModeler, an estimated maximum radius on the central circle of the target in test image must still be input, which may be inconvenient in practice.

**Figure 4. Experiment image: the better case**

4 Conclusion

We have presented an effective feature vector representing the coded targets, and nicely used the morphological operations for recognition of the targets. Although good recognition results are obtained, there are still some aspects to be improved. Firstly, more efficient thresholding methods are needed. Secondly, while the number of dilations needed in algorithm is easy to decide, automatic selection of the dilation number is expected. Finally, better speedup skills are expected to further improve the performance, especially compared to some existing commercial softwares.

**Figure 5. Experiment image: the worse case.**

Acknowledgment

This work is supported by National Natural Science Foundation of China (No. 60672135). The authors would like to thank the research group in Digital Inspection and Modeling Unit, Industrial Centre of The Hong Kong Polytechnic University for their useful discussions and constructive advices on this manuscript.

References

- [1] D. Akca and A. Gruen. Recent advances in least squares 3d surface matching. In K. H. Gruen, A., editor, *Optical 3-D Measurement Technique VII*, number 2, pages 197–206, Vienna, Austria, October 2005.
- [2] V. Estivill-Castro and M. E. Houle. Robust distance-based clustering with applications to spatial data mining. *Algorithmica*, 30(2):216–242, 2001.
- [3] H. K. M. Ester and J. Sander. A density-based algorithm for discovering clusters in large spatial databases with noise. In *Proceedings of the 2nd ACM SIGKDD*, pages 226–231, Portland, 1996.
- [4] J. Ma and Y. Xing. A kind of coded point and its recognition in reverse engineering. *Die and Mould Technology*, (2):52–54, 2003.
- [5] Y. B. Ma and Y. X. Zhong. A method for 3d scanning and reconstruction based on coded points. *Optical Technique*, 32(6):865–868, 2006.
- [6] W. N. Qian and A. Y. Zhou. Analyzing popular clustering algorithms from different viewpoints. *Journal of Software*, 13(8):1382–1394, 2002.
- [7] J. Serra. *Image Analysis and Mathematical Morphology*. Academic Press, 1982.